Arabian Journal of Chemistry (2021) **14**, 103190

King Saud University

Arabian Journal of Chemistry

www.ksu.edu.sa
www.sciencedirect.com

ORIGINAL ARTICLE

Spectroscopic, density functional theory, cytotoxicity and antioxidant activities of sulfasalazine and naproxen drugs combination

Yan Cao [a], Afrasyab Khan [b], Alireza Soltani [c,*], Vahid Erfani-Moghadam [d,e], Andrew Ng Kay Lup [f,g], Mehrdad Aghaei [c], Nafiseh Abdolahi [c,*], Mohsen Khalili [h], Marco Cordani [i], Hanzaleh Balakheyli [c], Samaneh Tavassoli [c], Ahmad B. Albadarin [j,*]

[a] *School of Mechatronic Engineering, Xi'an Technological University, Xi'an 710021, China*
[b] *Institute of Engineering and Technology, Department of Hydraulics and Hydraulic and Pneumatic Systems, South Ural State University, Chelyabinsk, Russian Federation*
[c] *Golestan Rheumatology Research Center, Golestan University of Medical Science, Gorgan, Iran*
[d] *Cancer Research Center, Golestan University of Medical Sciences, Gorgan, Iran*
[e] *Department of Medical Nanotechnology, School of Advanced Technologies in Medicine, Golestan, University of Medical Sciences, Gorgan, Iran*
[f] *School of Energy and Chemical Engineering, Xiamen University Malaysia, Jalan Sunsuria, Bandar, Sunsuria, 43900 Sepang, Selangor Darul Ehsan, Malaysia*
[g] *College of Chemistry and Chemical Engineering, Xiamen University, Xiamen 361005, Fujian, China*
[h] *Medical Cellular and Molecular Research Center, Golestan University of Medical Sciences, Gorgan, Iran*
[i] *Institute for Advanced Studies in Nanoscience (IMDEA Nanociencia), Madrid, Spain*
[j] *Department of Chemical Sciences, Bernal Institute, University of Limerick, Limerick, Ireland*

Received 19 February 2021; accepted 25 April 2021
Available online 30 April 2021

KEYWORDS

Anti-inflammatory drugs;
Antioxidant activity;
Toxicity;
Spectroscopy

Abstract In this study, we reported preparation and characterization of a new nano product consisting of the combination of two anti-inflammatory drugs: naproxen and sulfasalazine (Sulfoxen) where both are currently used for the treatment of inflammatory disorders. The nano combination product and its structural characterization were obtained by the Fourier transform infrared (FT-IR) spectroscopy, X-ray powder diffraction (XRPD), Thermogravimetric analysis (TGA),

* Corresponding authors.
E-mail addresses: alireza.soltani@goums.ac.ir (A. Soltani), n_abdolahi2002@yahoo.com (N. Abdolahi), ahmad.b.albadarin@ul.ie (A.B. Albadarin).

Peer review under responsibility of King Saud University.

Production and hosting by Elsevier

https://doi.org/10.1016/j.arabjc.2021.103190

Differential scanning calorimetry (DSC), Dynamic light scattering (DLS), Atomic force microscopy (AFM), and Field emission scanning electron microscopy (FE-SEM), respectively.

The hydrogen bonding between the COOH groups of naproxen (NPX) and sulfasalazine (SSZ) drugs were evaluated by the experimental and theoretical spectra. FESEM and AFM techniques represent that the most particles of Sulfoxen have a solid dense cubical or cuboidal structure and they also have size range of 50–100 nm. The objective was to prepare the nano-formulation of the Sulfoxen with improved antioxidant properties with respect to the two compounds administered separately. We have evaluated the anti-cancer effect of Sulfoxen in comparison to sulfasalazine and naproxen drugs on MCF-7 and KYSE30 cell lines. Interestingly, exposure of the zebrafishes to Sulfoxen (12.5 mM) did not exhibit lethal toxicity compared to the control groups. Therefore, Sulfoxen could contribute to more studies for the possible future clinical use.

1. Introduction

Drug combination is considered one of the most effective ways to improve therapeutic interventions in the treatment of many human diseases comprising cardiovascular disease, arthritis and cancer (Emily, 2017). However, optimizing for an efficacious combination is not an easy task. In the case of rheumatoid arthritis, the basic therapy includes the use of NSAIDs (nonsteroidal anti-inflammatory drugs) to alleviation of pain and detract inflammation along with disease modifying anti-rheumatic drugs (DMARDs) to save the joint functionality and to prevent damages in other tissues Baek et al., 2017. Naproxen (NSAID) and sulfasalazine (DMARD) are commonly prescribed as a combination of drugs to control the pain and inflammation and to simultaneously preventing further joint damage.

Sulfasalazine (SSZ) is a sulfa drug which is composed of 5-aminosalicylic acid (anti-inflammatory drug) and sulfapyridine (sulfanilamide antibacterial drug) by an azo bond. SSZ is frequently considered as a first-line treatment against a variety of auto-immune diseases, such as rheumatoid arthritis, inflammatory bowel disease (IBS), Crohn's disease and ulcerative colitis owing to its anti-bacterial and immunosuppressive properties Titchen, 2005; Sutherland et al., 2000; Hanauer et al., 2005; Bell and Habal, 2007. Naproxen (NAP) is a nonselective cyclooxygenase (COX) inhibitor and belonging to propionic acid class of NSAID that is normally used for the decrement of moderate to severe pain, fever, stiffness and inflammation caused by different types of arthritis, gout, tendinitis and bursitis (Diav-Citrin et al., 1998). NAP preferentially inhibits the activity of COX-1 (cyclooxygenase-1) and COX-2 (cyclooxygenase-2), which are predominately expressed in the gastrointestinal tract and in the sites of inflammation, respectively Schoen and Vender, 1989; Rodrigues et al., 2016; Erfani-Moghadam et al., 2020. Usually, 2–3 doses of naproxen and 4–6 doses of sulfasalazine are prescribed to rheumatologic patients every day. In order to minimize the number of drug admission in a day, combination drugs/fixed-dose combinations (FDCs) have become a necessity.

Recently, a number of methods have been expanded to design new dual stimuli-responsive nanoparticles able of efficient targeting delivery to reduce drug resistance and to enhance anti-inflammatory and anticancer activities (Feng et al., 2017; Mehta et al., 2019). Kłobucki and co-workers synthesized novel phosphatidylcholines comprising of the ibuprofen or naproxen moieties with high purities and good yields (Kłobucki et al., 2019). Their results indicated that phosphatidylcholine derivatives including 2-lysophosphatidylcholines carrying ibuprofen or naproxen moieties showed less toxic against human colon carcinoma Caco-2, porcine epithelial intestinal IPEC-J2, and human promyelocytic leukemia HL-60 cells compared to other phosphatidylcholine derivatives. Exploitation of the mixed of NSAIDs containing naproxen and naproxen sodium with sumatriptan (Treximet®[sumatriptan–naproxen]) for acute therapy of migraine has been evaluated by Khoury and Couch (Khoury and Couch, 2010). Lobmann et al. studied preparation and investigation of coamorphous drug/drug combination of a nonsteroidal and an anti-inflammatory drug (naproxen and γ-indomethacin) at molar ratios of 2:1, 1:1 and 1:2. The combinations were then analyzed by the XRPD, FTIR, and DSC Lobmann et al., 2011. Their results indicated that the combination of naproxen with indomethacin led to an amorphous form while it did not occur with naproxen alone. The FTIR spectra indicated the frequency shift caused by the molecular interactions of two drugs, forming a heterodimer.

The focus of the present study is to provide a single drug for rheumatoid arthritis obtained by the combination of SSZ and NAP with unaltered medicinal efficiency and enhanced therapeutic efficacy. The formulation procedure of Sulfoxen is discussed in details along with its characterization using several techniques. Moreover, the effect of combination in the inhibition of free radical production was further examined using the DPPH (2,2-diphenyl-1-picrylhydrazyl) radical scavenging activity, and its toxicity was elucidated by the zebrafish.

2. Materials and methodology

2.1. Materials

Sulfasalazine and naproxen drugs were purchased from Sigma-Aldrich at 99% purity. DPPH and BHT (butylated hydroxytoluene) compounds were procured from Sigma-Aldrich Ltd. (Germany). Also, methanol, 99% (CAS Number: 67-56-1), and acetone (CAS Number: 67–64-1), H_2SO_4 (CAS Number: 7664-93-9), $NaH_2PO_4{\bullet}H_2O$ (CAS Number: 10049–21-5), and $(NH_4)_6Mo_7O_{24}$ * $4H_2O$ (CAS Number: 12054-85-2) have been purchased from Merck. Doubly distilled water was used as solvent within the experiments.

2.2. Preparation of Sulfoxen nanocomplex

Sulfoxen nanoparticles were prepared by mixing the SSZ (50 mg in 20 mL methanol) and NAP (50 mg dissolved in 20 mL methanol) in 1:1 wt ratio with constant stirring (Fig. 1). The mixture was stirred at 40 ℃ for 12 h to obtain an orange color solution. Afterwards, the mixture was sonicated at 37 kHz, 80 W and 40 ℃ for 10 min. The mixture was centrifuged at 10000 rpm for 10 min. Finally, the orange color precipitate was filtered and carefully washed with cold methanol and dried at 50 ℃ in the oven for 24 h.

2.3. DPPH radical scavenging activity

A solution of 4.3 mg of DPPH in 3.3 mL of methanol was prepared in a test tube and protected from light by covering with aluminum foil (Tepe and Sokmen, 2007). A 150 µL of the solution was then taken and diluted up to 3 mL with methanol and then the absorbance was recorded at 517 nm by using UV–Visible spectrophotometer. This absorbance was assigned as the control. For the test and standard (std), the different concentrations of drugs were provided. For the assay, 150 µL of DPPH solution was added to 150 µL of the test or std solution and diluted up to 3 mL in methanol, the absorbance of the reaction mixture was determined after 30 min at 517 nm by UV–Vis spectrophotometer (methanol as blank). The percentage (%) scavenging activity was calculated by using the following equation:

$$\mathrm{DPPHscavengingactivity\%} = \frac{\mathrm{Absorbanceofcontrol} - \mathrm{Absrbanceofsample}}{\mathrm{Absorbanceofcontrol}}$$

2.4. Total antioxidant capacity

The total antioxidant capacity (TAC) is based on the decrement of Mo (VI) to Mo (V) by the compound and the subsequent formation of a green phosphate/Mo (V) complex at acidic pH (Prieto et al., 1999). An aliquot of 0.1 mL of sample solution and 1 mL of reagent solution (H_2SO_4 (0.6 M), $NaH_2PO_4 \bullet H_2O$ (28 mM), and $(NH_4)_6Mo_7O_{24}*4H_2O$ (4 mM)) was mixed in methanol and incubated at 95 ℃ for 90 min. After the reaction mixture cooled for 15 min at room temperature, the absorbance was determined at 695 nm. A typical blank solution included 1 mL of reagent solution and the convenient volume of the same solvent was prepared for the compound and it was incubated under the same conditions as the rest of the compounds.

2.5. FRAP assay

The FRAP (ferric reducing antioxidant power) assay of different parts was determined by the method of Yildirim et al. (Yildirim et al., 2001). The dried compound (125–1000 µg) in 1 mL of the corresponding solvent was blended with 2.5 mL of $K_3Fe(CN)_6$ [potassium ferricyanide; 10 g/L] and 2.5 mL of phosphate buffer (0.2 M), then the reaction mixture was allowed to react at 50 ℃ for 30 min. Then, 2.5 mL of TCA (trichloroacetic acid; 100 g l^{-1}) was added to the mixture and centrifuged at 1650 rpm for 10 min. Finally, 2.5 mL of the supernatant solution was blended with 2.5 mL of distilled water and 0.5 mL of $FeCl_3$ (1 µg/L) and the absorbance was determined at 700 nm. High absorbance indicates high reducing power.

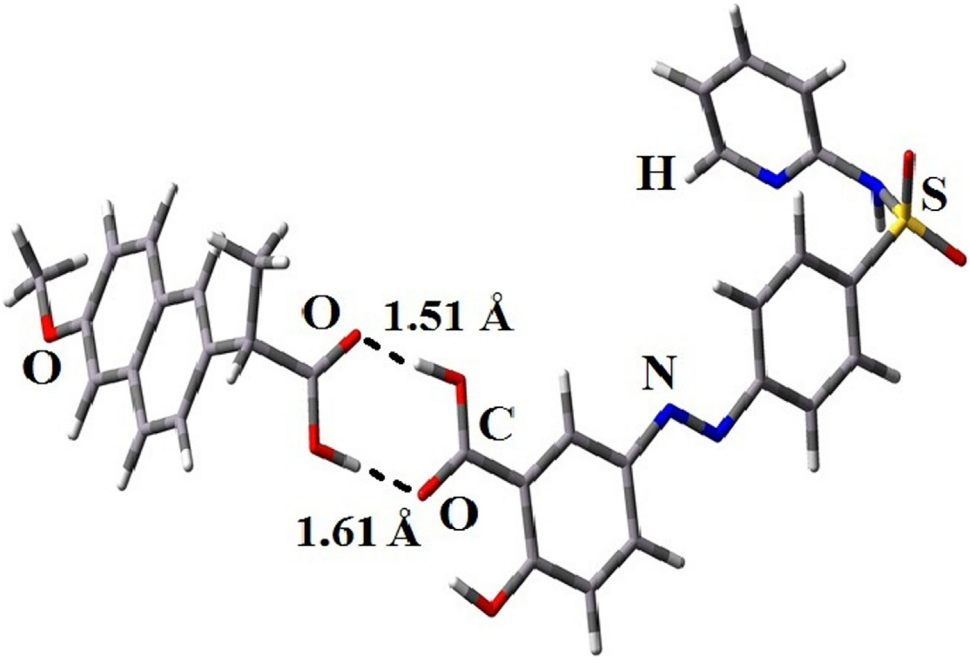

Fig. 1 Schematic diagram of the interaction between NAP and SSZ. The dashed lines between the COOH groups of both drugs represent the assumed H-bonding by the M06-2XD functional in methanol phase.

2.6. Fish preparing

Herein, zebrafish (*Danio rerio)* was selected as an experimental model. For acute toxicity bioassay 147 healthy, live specimens (~0.8 gr weight) of both sexes were used in this study. Fish were prepared from a breeding center, transferred to a workshop and adapted to the environment for one week. Fish were maintained in a stable environmental condition (Water temperature: 27.5 ± 0.5; hardness: 430 ± 25; pH: 7.5) during the adaptation. They were fed on a commercial diet twice daily. Feeding was stopped 24 h before experimenting.

2.7. Range finding test

A range finding test was performed to characterize the range of the substance according to OECD 203. The highest concentration of test substance to use in the range-finding test was 12.5 mM and the lowest one was 2 mM. Fish in the test and control chambers were monitored periodically to remove possible mortality.

2.8. UV–Vis analysis

UV–Vis spectra of SSZ, NAP and Sulfoxen samples in methanol were recorded in an (UV–Vis machine name) with a spectral range from 200 nm to 700 nm and spectral resolution of 1 nm. Quartz cuvettes were filled with 3 mL of each sample and a quartz cuvette with 3 mL of methanol was used as blank sample. Each spectrum was recorded in triplicate.

2.9. Physicochemical characterization

FT-IR spectroscopy (JASCO680 plus FT-IR spectrophotometer, Perkin-Elmer) and Raman (SENTERRA, BRUKER, Germany) were utilized for evaluating the combination. The rate of decomposition of free SSZ and NAP and their combined complex were evaluated using TGA (thermal gravimetric analysis) (Q50, Thermal Analysis -TA) with the experimental conditions of scanning from 25 to 700 °C under argon flow at a heating rate of 20°C/min. Sample was also scanned from 25 to 700 °C at 20 °C/min in The LINSEIS Differential Scanning Calorimeters (DSC) to detect for thermal induced phase transition or decomposition of sample. The crystallinity of the complex was evaluated using XRPD analysis. Particle size of nanocomplex was also analyzed using FE-SEM (DSM-960A, Zeiss Company).

2.10. Cell toxicity assay

Cell toxicity MTT assay was accomplished with a tetrazolium compound 3-(4,5-dimethylthiazol-2-yl)-2,5-diphenyltetrazolium bromide (MTT) provided by a Bio-IDEA MTT assay Kit. The MCF-7 and KYSE30 cell lines were cultured as a monolayer in a 25-cm^2 flask containing DMEM enriched with a mixture of 100 U/mL penicillin and 100 μg/mL streptomycin, and 10% FBS. The cells were preserved in a 95% humidity and 5% CO_2 at 37 °C incubator. Then, the cell morphology was determined by an inverted microscope. Ultrasonic dispersion and a vigorous vortex of the sulfasalazine-naproxen combination colloidal stock was done, serial dilutions of treatments were provided ranging from 5 to 250 μM, and their cytotoxic effects were tested on standard cell lines using MTT assay. Untreated cells served as the control. The cells were exposed to MTT (0.5 mg/mL in phosphate buffered saline) for four hours at 37 °C, the medium was eliminated. The absorbance measurement was computed at 490 nm, and then the cell viability percentage was compared with untreated control cells.

2.11. Theoretical method

All calculations were performed via the GAMESS package (Schmidt et al., 1993) at the density functional theory (DFT) level using the hybrid M06-2X exchange functional augmented with an empirical dispersion term (M06-2X-D) (Ghasemi et al., 2019). The optimized molecules were further subjected to the calculations for harmonic vibrational frequencies at the M06-2X/6-311 + G** level of theory. The excited states are determined with TDDFT (time-dependent density functional theory). The functional used in TDDFT calculation is M06-2X with 6-311 + G** basis set. Vibrational frequencies were also evaluated by the M06-2X/6-311 + G** level of theory to determine the reliability of the relaxed structures, in addition to study assign experimental data.

3. Results and discussion

3.1. Characterization of complex

3.1.1. UV–Vis spectra and interaction energies

As displayed in Fig. 2, the ultraviolet–visible absorption spectra (UV–visible) of the SSZ, NAP and Sulfoxen compounds in methanol were measured. NAP shows broad band at 332 nm due to π-π* transition of naphthalene ring and 244 and 272 nm possibly owing to the n-π* transitions of carboxyl and ether groups in the presence of polar solvent Perez et al., 2015. SSZ also shows two peaks at 253 and 359 nm which are respectively attributed to n-π* transition of carboxylic group and π-π* transition of benzene ring (Fig. 2) (Ghashim, 2012). Sulfoxen compound shows a slight hypsochromic shift in the UV–Vis band of carboxyl group at 240 nm. Formation of Sulfoxen involves hydrogen bonding between the two drugs at carboxyl group which prevents the conjugation of carboxylate ions causing the conjugation system to increase in energy gap. Absorbance band of Sulfoxen

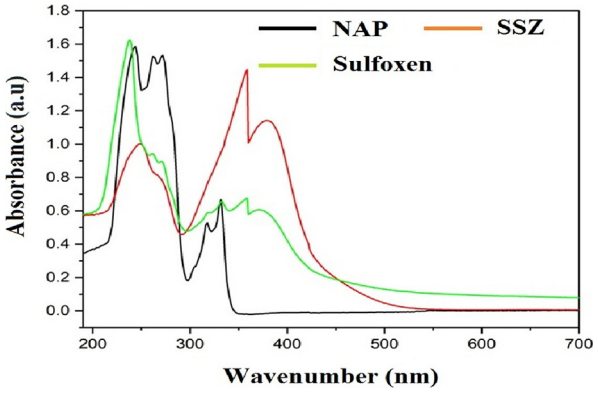

Fig. 2 UV–visible spectra of NAP, SSZ and coamorphous (1:1) Sulfoxen.

between 300 nm and 500 nm is approximately equivalent with the sum of NAP and SSZ absorbance due to aromatic rings with 1:1 wt ratio. Based on theoretical modeling of UV–Vis absorption, Sulfoxen compound represents a strong absorption peak at 220 nm with oscillator strength of 0.911 and a strong absorption peak at 312 nm with oscillator strength of 1.02 in methanol phase which are in corroboration with the UV–Vis spectral data. In UV–Vis absorption spectra of pure SSZ demonstrates the main band maximum is observed at 226 and 369 nm while the NPX drug shows the main band maximum is observed at 221 and 286 nm.

We also evaluated the interaction energy between NAP and SSZ through carboxyl (–COOH) groups by the M06-2XD functional. Fig. 1 represents the formation of hydrogen bonding between carboxyl groups of both drugs in methanol phase. The estimated value of the interaction energy is −14.89 kcal/-mol. The most substantial geometrical variations in the interaction process are inconsiderable increase in C-O bond length of SSZ from 1.224 Å to 1.244 Å and little increment of C-O bond length of NAP from 1.209 Å to 1.229 Å.

3.1.2. FT-IR and Raman spectra

FT-IR spectra of the free SSZ, NAP, and its combination complex (Sulfoxen) were recorded in the range of 400–4000 cm^{-1}. The FT-IR spectra of free SSZ and NAP drugs have a strong intensity band at 1638 and 1629 cm^{-1} range due to υ(C = C). Whilst the Sulfoxen drug shows a weak IR mode at 1460 cm^{-1}. The phenolic C-O stretching mode from 1167 and 1141 cm^{-1} in the free SSZ and NAP drugs shifted to 1111 cm^{-1} in the combination drug M.G. Abd EL-WAHED, M.S. REFAT, S.M. EL-MEGHARBEL, , 2009; Bhise et al., 2008. The theoretical result of the combination drug indicates that the phenolic C-O stretching mode is shifted to lower wavenumber (1108 cm^{-1}). Presence of the OH group showed a shift for the δ(OH) in-plane bending from 1394 and 1362 cm^{-1} in the free SSZ and NAP drug to 1354 cm^{-1} in the Sulfoxen compound.

FT-IR spectrum of naproxen (data shown in Table 1) displays fairly sharp bands at 1236, 1362, 3188, and 1677 cm^{-1} in turn due to C-O stretching vibration, CH_3 bending, OH stretching band, ν(C = O) stretching mode. Meanwhile, the modes at 2926–3140 cm^{-1} illustrate C-H aromatic and aliphatic stretching vibrations (Srivastava et al., 2018). The free SSZ and NAP drugs indicate respectively the OH stretching vibrations at 3315 and 3188 cm^{-1}. In the combination drug, this characteristic band shifts to 3454 cm^{-1} with a reduced intensity which is assigned to the formation of intermolecular hydrogen bonding. The result of the calculated theoretical harmonic frequency shows abroad band in the region of 3540 cm^{-1} which can attribute to hydroxyl groups (OH) in the combination drug, which is close to the experimental result obtained. Abd El-Wahed and co-workers reported the IR spectrum of sulfasalazine that indicated a medium broadband at 3439 cm^{-1}, assigning the OH stretching vibration of the phenolic and carboxylic OH groups M.G. Abd EL-WAHED, M.S. REFAT, S.M. EL-MEGHARBEL, , 2009.

FT-IR spectrum indicates that the SO_2 group in the combination drug leads to emerging strong bands at 1364 cm^{-1} stemming from the symmetric vibration, whereas this group observed at 1360 cm^{-1} in the free SSZ drug. Based on the FT-IR spectrum in the combination drug, the medium band at 1607 cm^{-1} is related to the aromatic ring skeleton stretching vibration of benzene ring: υ(C = C), which is comparable to theoretical calculations (1632–1663 cm^{-1}). In addition, the theoretical result on the combination drug represents that the υ(C = O) vibration observed in region between 1694 cm^{-1} and 1807 cm^{-1}, which is comparable to experimental data (1702–1761 cm^{-1}). The vibration bands at 2864 and 2922 cm^{-1} are assigned to C-H aromatic ring and asymmetric stretching vibration of the methyl group: $\upsilon_{asym}(CH_3)$, respectively.

We studied the Raman analysis for the combination of sulfasalazine with naproxen in the range of 2500–400 cm^{-1}. The Raman spectrum of naproxen shows sharp peaks at 400, 560, 700, 750, 860, 1170, 1400, 1420, 1480, 1580 and 1620 cm^{-1} whereas sulfasalazine shows sharp peaks at 630, 800, 1110, 1150, 1250, 1300, 1400, 1450, 1490 and 1580 cm^{-1}. The major peaks in the combined drug are located at 1149, 1396, 1444, 1589, and 1742 cm^{-1} (Fig. 3). Several peaks in the absorbance range of 400–1000 cm^{-1} were significantly reduced in intensity which indicates the reduction in vibration energies associated with C-C and C-O bonds, ring deformation and skeletal vibration.

3.1.3. Thermal analysis

The blue curve in Fig. 4 is the DSC curve which measures temperature differences while the green curve is TG curve which measures weight loss of sample. To avoid confusion on the blue curve as DTG curve, the caption of Fig. 4 was updated for further distinction on TG and DSC curves. We found that the naproxen drug completely decomposes (99%) within the temperature range of 150–480 °C with a main mass loss at 266.93 °C based on TGA curve. Zayed et al. proposed that the thermal decomposition of naproxen occurs due to three fragmentations: carboxyl at 150–170 °C, ethyl at 210–280 °C and methoxyl at 400–480 °C (Zayed et al., 2017). The differential scanning calorimetry (DSC) analysis of the naproxen also represents endothermic and exothermic mass loses involved in the decomposition of this drug. Moreover, the sulfasalazine drug decomposes at 279 °C resulting in the mass losses of $C_4H_6N_4SO_3$ (47.20%,) and $C_2H_8O_2$ (16.50%) as the organic moieties which are endothermic mass losses (Refat et al., 2011). Combination drug which is comprised of those two drugs shows a similar behavior to the precursors with some negative

Table 1 FT-IR data for the SSZ and NAP and its combination complex.

ν(OH)	ν(C = C)	$\nu_{sym.}$(C-C)	ν(N = N)	δ(OH)	ν(C = O)	$\nu_{asym.}(SO_2)$	ν(C-O)	**Compound**
3454	1607	1458	1577	1354	1702–1761	1364	1111	Sulfoxen
3315	1638	1487	1587	1394	1675	1360	1167	SSZ
3188	1629	1481	–	1362	1677	–	1141	NAP

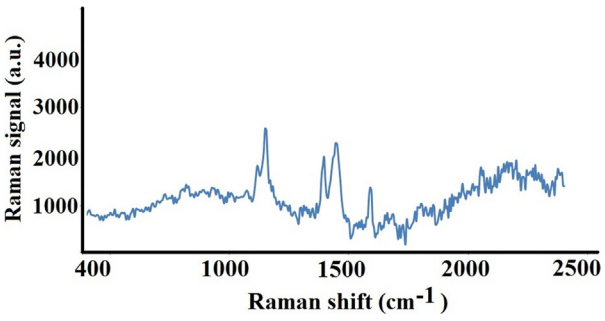

Fig. 3 Raman spectrum of the Sulfoxen compound.

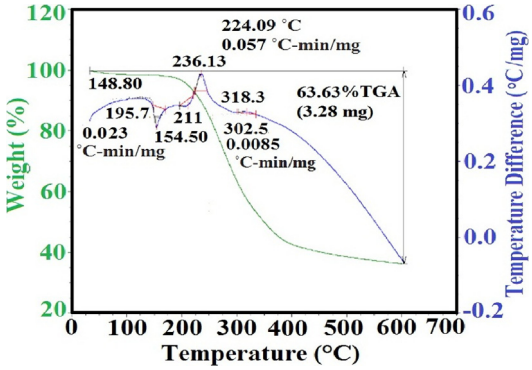

Fig. 4 Thermal analysis of Sulfoxen compound: TG curve (Green) and DSC curve (Blue).

shifts in the temperature values. The thermal analysis of the combination drug was performed in a temperature range of 0–600 °C using a Universal V4.5A TA Instrument.

The TGA curve stands for couple of steps in the mass loss with the main mass loss of 63.63% placed between 200 and 400 °C (Soliman, 2006). The DSC curve also represents an exothermic (at 154.5 °C) and three endothermic (211, 236 and 318 °C) processes occurring within thermal decomposition of the combination drug (Fig. 4). These results illustrate that thermal decomposition of the combination drug occur in four consecutive steps. The DSC curve further confirmed that the mass loss of 63.73% (3.285 mg) is occurred at 200–400 ℃. DSC profile represents three endothermic peaks, the first at 352 K corresponding to the melting of the combined drug, the second at 600 K assigns to the dehydration and decomposition of the sulfoxen compound and the third board endothermic peak related to the final decomposition of the sulfoxen.

3.1.4. XRPD analysis

XRPD analysis was done in order to obtain further evidence about the structure and lattice dynamics of the combination drug. The effect of temperature on drugs can be investigated by observing the alteration of lattice parameters and the reactions of drug Shen et al., (2018). The melting point of USP Naproxen Reference Standard was 154.4–156.2 °C [lit. 155.3 °C 3)], and that of USP Sulfasalazine Reference Standard was 260–265 °C [lit. 262.5 °C (12)]. The XRPD pattern of the pure SSZ is consistent with those reported in the literature da Costa et al., 2015; Rajesh et al., 2011 and exhibits well-defined crystalline structure with characteristic signals at 11.9°, 15.1°, 23.1°, and 27.6°. The XRPD pattern of the pure NAP have the distinct peaks at 2θ: 6.5°, 12.4°, 16.6o, 19o, 20o, 22.5o, 24o and 28.5o (Javadzadeh et al., 2010). As displayed in Fig. 5, the XRPD pattern obtained for the Sulfoxen indicates high crystallinity of the combination drug. The XRPD analysis of the combination drug presents reflecting peaks at 27.50, 31.90, 45.50, 53.95, 56.50 and 66.32° attributing the (111), (200), (220), (311), (222), and (400) crystal planes respectively. Shown in Fig. 5, the last four XRPD peaks were attributed to the heterodimer structure of Sulfoxen with the coformers via strong hydrogen bonds between NAP and SSZ. The presence of heterodimer in the crystal lattice resulted in substantial discrepancy in the crystal structure of Sulfoxen have profound impact on drug features.

3.1.5. FESEM analysis

The morphology, size, shape and elemental composition of the combination drug (Sulfoxen) are displayed in Fig. 6. FESEM image of the sulfoxen nanoparticles demonstrated that the nanoparticles have a solid dense cubical or cuboidal structure and not aggregated. As can be seen in Fig. 6, Sulfoxen nanoparticles represent the almost spherical shape with the mean particle size of 50–100 nm. EDX spectrum of combination drug nanoparticles is shown in Fig. 6. The EDX spectrum represents the attendance of C (56.36%), O (17.26%), S (4.61%), and N (5.62%) in the combination drug. Elemental maps are presented in Fig. 7 and indicated that the entire particle surface consists of C, N, and O.

3.1.6. AFM and DLS analyze

In Fig. 8(a), AFM analysis indicated that the size of the the nano combination products ranging from 50 to 150 nm with near cubical or cuboidal shapes. AFM image of combination products presents the height of nanoparticles to be 20 nm as shown in Fig. 8. Dynamic light scattering (DLS) assay performed to define the physical features of combination products

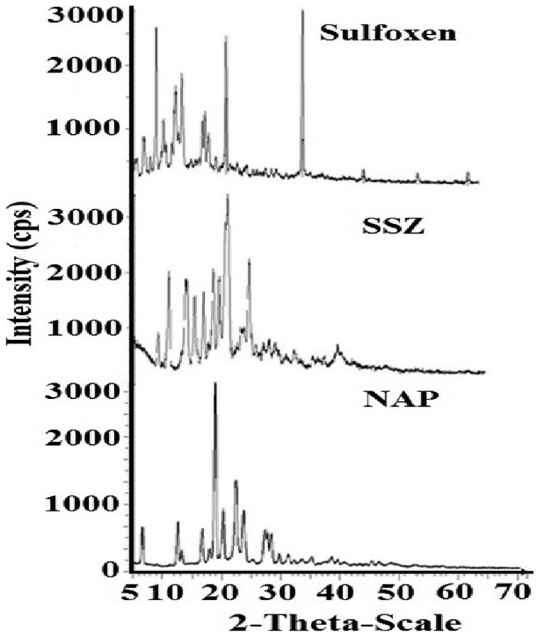

Fig. 5 XRPD patterns of the SSZ, NAP and Sulfoxen complex.

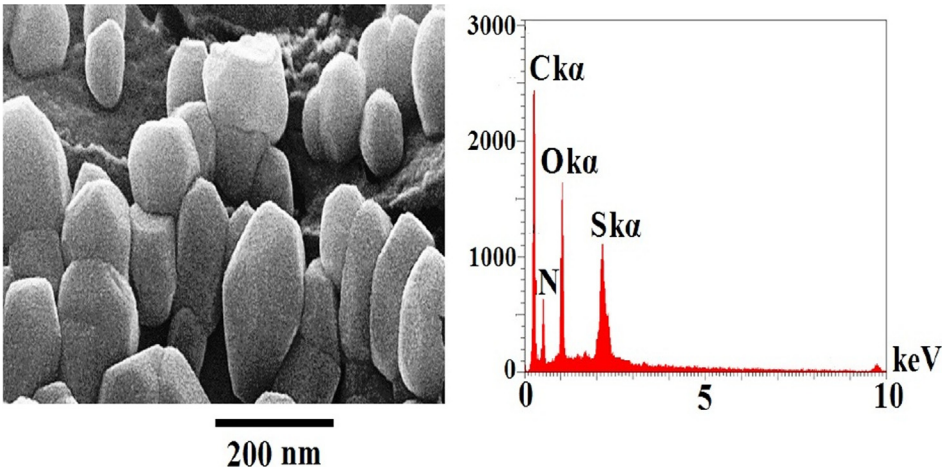

Fig. 6 FESEM image and EDX spectrum of Sulfoxen compound.

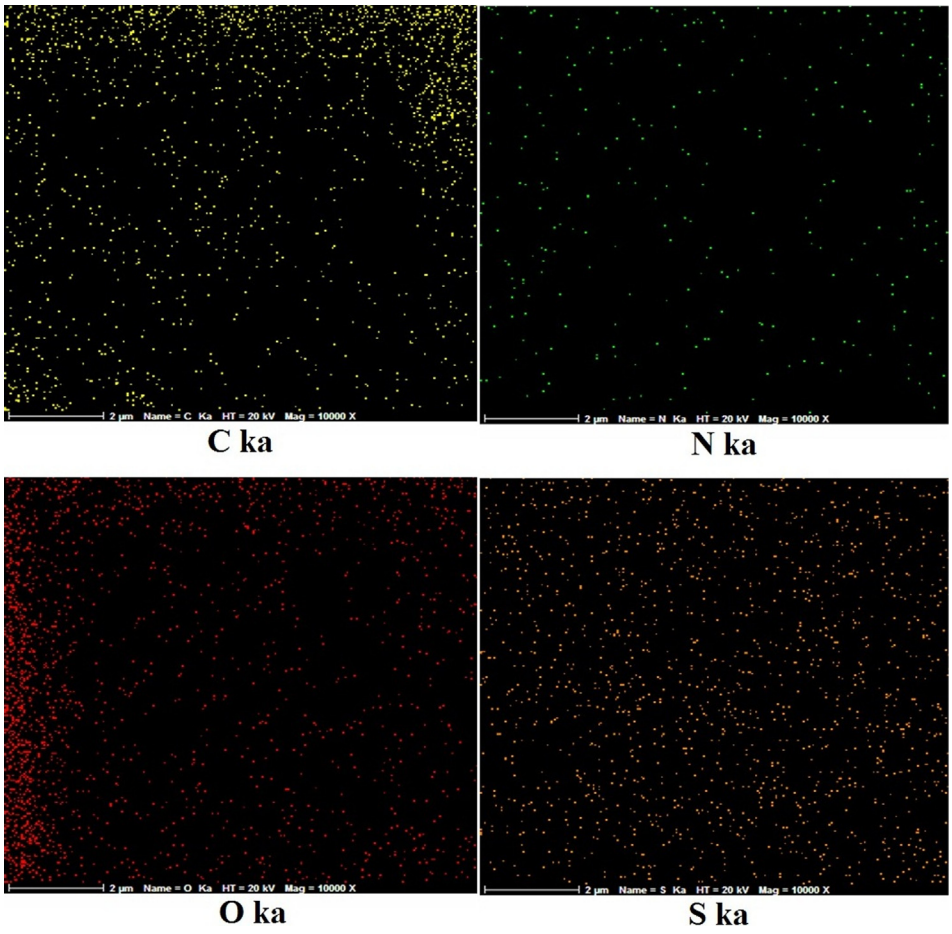

Fig. 7 EDX elemental map for different elements of the Sulfoxen compound.

(Fig. 6(b)). The mean size of Sulfoxen nanoparticles was analyzed with a value of 157.7 ± 45.7 nm.

3.2. Anti-oxidizing activity

The TAC and FRAP (Abdolahi et al., 2018) of the tested compounds, containing SSZ, NPX, and sulfoxen nanoparticles have been determined by DPPH assay. The obtained results in Table 2 represent the effect of each of these molecules on the decrement of oxidation, which is presented by the concentration index required for 50% inhibitory IC_{50}. The highest antioxidant activity of the Sulfoxen was found to be 73.0% inhibition at concentration of 100 mg/mL, while highest antioxidant activity for the pure sulfasalazine and naproxen

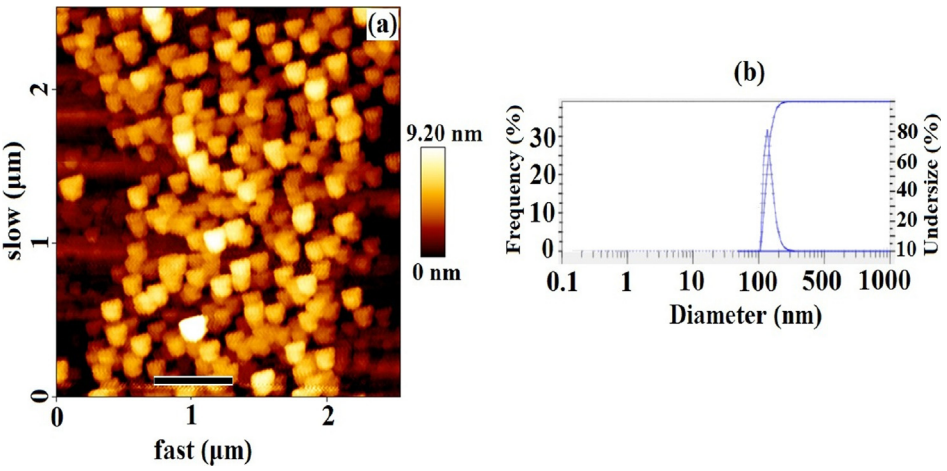

Fig. 8 AFM (a) and DLS (b) images of sulfoxen compound.

Table 2 IC_{50} value of Sulfoxen in different free radical scavenging tests.

IC_{50} (mg/mL)			
DPPH radical scavenging	Total assay	FRAP	Sample
0.76	62.0	27.0	Sulfoxen
1.03	99.0	27.0	SSZ
3.46	12.47	08.3	NAP

are found to be 23% and 1%, respectively. The result represents the sulfoxen has a higher antioxidant capacity than pure samples of SSZ, and NPX. Sulfoxen has IC_{50} values way below the average of IC_{50} values of sulfasalazine and naproxen, indicating that the drug combination does provide synergistic effect instead of additive property. See Table 3

For pure drug samples, NAP has lower reducing power than SSZ as the former has naphthalene and carboxyl group as the stronger conjugated system to provide better redox resistance. With the drug combination, conjugation of carboxyl groups in both NAP and SSZ were both prevented due to intermolecular hydrogen bonding between carboxyl groups. This resulted in the weakened conjugated system of the overall structure thus significantly improve the reducing power of sulfoxen. The results demonstrated that the best oxidation inhibitory effect between the three test specimens with all three methods is to evaluate the composition of naproxen-sulfasalazine, which has the lowest concentration used for inhibiting the specific percentage (IC_{50}). This amount of inhibition is generally lower than the synthetic antioxidant effect of BHT.

Table 3 Compared IC50s of free NPX and SSZ in two cancer cell lines.

Cell lines	NPX (μM)	SSZ (μM)	Sulfoxen (μM)
MCF-7	2300	775	Not observed below the 300
KYSE30	1900	500	Not observed below the 300

3.3. Cell toxicity studies

We evaluated cytotoxic effects of Sulfoxen nanoparticle on KYSE30 and MCF-7 cell lines in compared to NPX and SSZ alone. For MCF-7 cell line, IC_{50} values of free naproxen and sulfasalazine were 2300 and 775 μM. For KYSE30 cell line, IC_{50} values of free naproxen and sulfasalazine were 1900 and 500 μM Deb et al., 2014; Narang et al., 2007. We did not observe a significant toxicity for Sulfoxen nanoparticles until 300 μM concentration. We previously demonstrated that ST8MNV nanoformulation (Squalene (S) and Tween 80 (T8) Micellar/Niosomal Vesicles) significantly improved solubility of naproxen which leads more efficient anticancer property of naproxen Erfani-Moghadam et al., (2020). This formulation also improves the bioavailability of sulfasalazine and promotes its effectiveness through the induction of cancer cells apoptosis (Aghaei et al., 2021).

3.4. In vivo toxicity against zebra fish

We explored the use of zebrafish as an alternative model for toxicity testing of sulfoxen compared to the free sulfasalazine and naproxen drugs in order to provide an *in vivo* assessment of combined effects of drugs at an earlier stage in drug discovery. In the course of resistance test, Sulfoxen compound showed no toxicity towards zebrafish at concentrations between 1 millimolar (mM) to 12.5 mM after 120 h of treatment. Therefore, the results of the test showed that zebrafish is not affected during the administration of this substance in our determined doses range, suggesting their safety for potential clinical use.

4. Conclusions

In order to provide a unique efficient nanodrug for the treatment of inflammatory diseases (e.g. rheumatoid arthritis), in the present study we prepared and characterized a nanoformulation consisting in the combination of naproxen and sulfasalazine (Sulfoxen) employing a variety of techniques including FT-IR spectroscopy, XRPD, and FE-SEM. We demonstrated that sulfoxen has an improved antioxidant activ-

ity compared to the administration of separate drugs. Using zebrafish as *in vivo* model for testing toxicity of Sulfoxen, we also report the absence of toxic side effects in the conditions of our study, suggesting its safety for a potential clinical use. Therefore, this nano-combined product offers great potentiality for future *in vitro* and *in vivo* investigations and may be of interest to the community for potential clinical anti-inflammatory and anticancer activities.

Declaration of Competing Interest

The authors declare that they have no known competing financial interests or personal relationships that could have appeared to influence the work reported in this paper.

Acknowledgements

We gratefully acknowledge financial support from Golestan University of Medical Science (Research Project Grant No. 970308036).

References

Emily, J., 2017. Bartley, Shreela Palit, Roland Staud, Predictors of Osteoarthritis Pain: The Importance of Resilience. Curr. Rheumatol. Rep. 19 (9), 57.

Baek, J.-S., Yeo, E.W., Lee, Y.H., Tan, N.S., Joachim Loo, S.C., 2017. Controlled-release nanoencapsulating microcapsules to combat inflammatory diseases. Drug Design, Develop. Therapy 11, 1707–1717.

Titchen, Thirza, 2005. Noel Cranswick1, Sean Beggs, Adverse drug reactions to nonsteroidal anti-inflammatory drugs, COX-2 inhibitors and paracetamol in a paediatric hospital. Br. J. Clin. Pharmacol. 59 (6), 718–723.

Sutherland, L., Roth, D., Beck, P., May, G., Makiyama, K., 2000. Cochrane Database Syst. Rev. CD000543.

Hanauer, S.B., Sandborn, W.J., Kornbluth, A., Katz, S., Safdi, M., Woogen, S., Regalli, G., Yeh, C., Smith-Hall, N., Ajayi, F., 2005. Am. J. Gastroenterol. 100, 2478.

Bell, C.M., Habal, F.M., 2007. Am. J. Gastroenterol. 92, 2201.

Diav-Citrin, O., Park, Y.H., Veerasuntharam, G., Polachek, H., Bologa, M., Pastuszak, A., Koren, G., 1998. Gastroenterology 114, 23.

Schoen, R.T., Vender, R.J., 1989. Mechanisms of nonsteroidal anti-inflammatory drug-induced gastric damage. Am. J. Med. 86 (4), 449–458.

Rodrigues, M.R., Lanzarini, C.M., Ricci-Junior, E., 2016. Preparation, in vitro characterization and in vivo release of naproxen loaded in poly-caprolactone nanoparticles. Pharm. Dev. Technol. 16 (1), 12–21.

Erfani-Moghadam, V., Aghaei, M., Soltani, A., Abdolahi, N., Ravaghi, A., Cordani, M., Shirvani, S., Moazen Rad, S., Balakheyli, H., 2020. ST8 micellar/niosomal vesicular nanoformulation for delivery of naproxen in cancer cells: Physicochemical characterization and cytotoxicity evaluation. J. Mol. Struct. 1211, 127867.

Feng, L., Wang, Y., Luo, Z., Huang, Z., Zhang, Y., Guo, K., Ye, D., 2017. Dual Stimuli-Responsive Nanoparticles for Controlled Release of Anticancer and Anti-inflammatory Drugs Combination. Chem. Eur. J 23 (39), 9397–9406.

Mehta, Chetan Hasmukh, Narayan, R., Aithal, G., Pandiyan, S., Bhat, P., Dengale, S., Shah, A., Yogendra Nayak, U., Garg, S., 2019. Molecular simulation driven experiment for formulation of fixed dose combination of Darunavir and Ritonavir as anti-HIV nanosuspension. J. Mol. Liquids 293, 111469.

Kłobucki, M., Urbaniak, A., Grudniewska, A., Kocbach, B., Maciejewska, G., Kiełbowicz, G., Ugorski, M., Wawrzeńczyk, C., 2019. Syntheses and cytotoxicity of phosphatidylcholines containing ibuprofen or naproxen moieties. Sci. Rep. 9, 220.

Khoury, C.K., Couch, J.R., 2010. Sumatriptan–naproxen fixed combination for acute treatment of migraine: a critical appraisal. Drug Des., Develop. Therapy 4, 9–17.

Lobmann, K., Laitinen, R., Grohganz, H., Gordon, K.C., Strachan, C., Rades, T., 2011. Coamorphous Drug Systems: Enhanced Physical Stability and Dissolution Rate of Indomethacin and Naproxen. Mol. Pharmaceut. 8, 1919–1928.

Tepe, B., Sokmen, A., 2007. Screening of the antioxidative properties and total phenolic contents of three endemic Tanacetum subspecies from Turkish flora. Bioresource Technol. 98, 3076–3079.

Prieto, P., Pineda, M., Aguilar, M., 1999. Spectrophotometric quantitation of antioxidant capacity through the formation of a phosphomolybdenum complex: specific application to the determination of vitamin E. Anal. Biochem. 269, 337–341.

Yildirim, A., Mavi, A., Kara, A.A., 2001. Determination of antioxidant and antimicrobial activities of Rumex crispus L. extracts. J. Agr. Food Chem. 49, 4083–4089.

Schmidt, M.W., Baldridge, K.K., Boatz, J.A., Elbert, S.T., Gordon, M.S., Jensen, J.H., Koseki, S., Matsunaga, N., et al, 1993. J. Comput. Chem. 11, 1347.

Ghasemi, A.S., Ramezani Taghartapeh, M., Soltani, A., Mahon, P.J., 2019. Adsorption behavior of metformin drug on boron nitride fullerenes: thermodynamics and DFT studies. J. Mol. Liq. 275, 955–967.

Perez, Martin, Concu, Riccardo, Ornelas, Mariana, Natalia, M., Cordeiro, D.S., Azenha, Manuel, Fernando Silva, A., 2015. Measurement artifacts identified in the UV–vis spectroscopic study of adduct formation within the context of molecular imprinting of naproxen, 153, 661–668.

Ghashim, L.L., 2012. Synthesis and Characterization of a New Complexo Cobalt (III) Sulfasalazine Hydroxamate. J. Al-Nahrain Univ. 15 (4), 82–90.

ABD EL-WAHED, M.G., REFAT, M.S., EL-MEGHARBEL, S.M., 2009. Spectroscopic, thermal and biological studies of coordination compounds of sulfasalazine drug: Mn(II), Hg(II), Cr(III), ZrO(II), VO(II) and Y(III) transition metal complexes. Bull. Mater. Sci., 32, 205–214.

Bhise, K.S., Dhumal, R.S., Paradkar, A.R., Kadam, S.S., 2008. Effect of drying methods on swelling, erosion and drug release from chitosan-naproxen sodium complexes. AAPS Pharm. Sci. Tech. 9, 1–12.

Srivastava, P., Singh, K., Verma, M., Sivakumar, S., Patra, A.K., 2018. Photoactive platinum(II) complexes of nonsteroidal anti-inflammatory drug naproxen: Interaction with biological targets, antioxidant activity and cytotoxicity. Eur. J. Med. Chem. Eur. J. Med. Chem. 144, 243–254.

Zayed, M.A., Hawash, M.F., El-Desawy, M., El-Gizouli, A.M.M., 2017. Investigation of naproxen drug using mass spectrometry, thermal analyses and semi-empirical molecular orbital calculation. Arabian J. Chem. 10, 351–359.

Refat, M.S., El-Korashy, S.A., El-Deen, I.M., El-Sayed, S.M., 2011. Experimental and spectroscopic studies of charge transfer reaction between sulfasalazine antibiotic drug with different types of acceptors. Drug Test. Anal. 3, 116–131.

Soliman, A.A., 2006. Spectral and thermal study of the ternary complexes of nickel with sulfasalazine and some amino acids. Spectrochimica Acta Part A 65, 1180–1185.

Shen, Y.-J., Zhang, Y.-L., Gao, F., Yang, G.-S., Lai, X.-P., 2018. Influence of Temperature on the Microstructure Deterioration of Sandstone. Energies 11, 1753.

da Costa, M.A.B., Villa, A.L.V., Barros, R.C.S.A., Ricci-Júnior, E., dos Santos, E.P., 2015. Development, characterization and evaluation of the dissolution profile of sulfasalazine suspensions. Braz. J. Pharm. Sci. 51, 449–459.

Rajesh, A., Sangeeta, A., Lamba, H.S., Anil, B., Sandeep, K., 2011. Effect of the preparation of solid dispersion method on the solubility and crystallinity of sulfasalazine. Int. Res. J. Pharm. 2, 200–206.

Javadzadeh, Y., Ahadi, F., Davaran, S., Mohammadi, G., Sabzevarid, A., Adibki, K., 2010. Preparation and physicochemical characterization of naproxen–PLGA nanoparticles. Colloids Surf. B: Biointerfaces 81, 498–502.

Abdolahi, N., Soltani, A., Mirzaali, A., Soltani, S., Balakheyli, H., Aghaei, M., 2018. Antibacterial and Antioxidant Activities and Phytochemical Properties of Punica granatum Flowers in Iran. Iran J. Sci. Technol. Trans. Sci. 42, 1105–1110.

Deb, J., Majumder, J., Bhattacharyya, S., Sankar Jana, S., 2014. A novel naproxen derivative capable of displaying anti-cancer and anti-migratory properties against human breast cancer cells. Deb et al. BMC Cancer 14, 567.

Narang, V.S., Pauletti, G.M., Gout, P.W., Buckley, D.J., Buckley, A. R., 2007. Sulfasalazine-Induced Reduction of Glutathione Levels in Breast Cancer Cells: Enhancement of Growth-Inhibitory Activity of Doxorubicin. Chemotherapy 53, 210–217.

Aghaei, M., Erfani-Moghadam, V., Soltani, A., Abdolahi, N., Cordani, M., Moazen Rad, S., Balakheyli, H., 2021. Non-Ionic Surfactant Micelles/Vesicles as Novel Systems to enhance solubility of Sulfasalazine: Evaluation of the Physicochemical and Cytotoxic Properties. J. Mol. Struct. 1230, 129874.